Botanical Studies (2006) 47: 279-292.

Study on laminar hydathodes of *Ficus formosana* (Moraceae) II. Morphogenesis of hydathodes

Chyi-Chuann CHEN and Yung-Reui CHEN*

Institute of Molecular and Cellular Biology, National Taiwan University, Taipei, TAIWAN

(Received September 16, 2005; Accepted February 16, 2006)

Abstract. The spatial and temporal morphogenesis of laminar hydathodes in *Ficus formosana* Maxim. f. *shimadai* Hayata was examined at light and electron microscopic levels. Four main stages of hydathode development, including initiation, cell division, cell elongation and differentiation, and maturation, can be identified. In the early stage of leaf development, the initial cells occur in the nearby region of a giant trichome. In the cell division stage, epidermal initial cells undergo anticlinal division to form epidermal cells and water pores. Subepidermal initial cells undergo anticlinal and periclinal divisions to produce a group of cells which further differentiate into epithem, tracheid cells, and a sheath layer of hydathodes. During the cell elongation and differentiation stage, epithem cells grow into lobe-shaped cells and separate from adjacent cells through schizogeny, caused by the arrangement of the cortical microtubules, the secretion of digesting enzymes acting on the cell wall, and the force and tension induced by cell growth. These factors not only cause the formation of lobed cells, but also enlarge the intercellular spaces of the epithem. The lobed epithem cells increase the contact regions between the cell and their environment. During the final stage, tracheids gradually mature within the epithem and develop their conductive function, by which water passes through the way between vein-ends and water pores to produce guttation. The pathway of epithem directional differentiation and maturation starts at the water pores and moves toward the region of vein-ends. Guttation is associated with the maturation of water pores, the epithem cells, and tracheid-ends. This study provides anatomical data of developmental events as a structural basis for understanding the hydathode's function.

Keywords: Epithem; *Ficus formosana* Maxim.; Hydathodes; Morphogenesis; Schizogenous intercellular space; Water pore.

INTRODUCTION

Guttation, the process of liquid water exudation, is driven by the hydrostatic pressure, handles the water equilibrium in xylem, and improves root absorption of nutrient solutes for plant development (Pedersen, 1993; Tanner and Beevers, 2001; de Boer and Volkov, 2003). Guttated solution is exuded through the hydathodes out of leaves. Generally, hydathodes are classified as either epidermal or epithemal hydathodes (Haberlandt, 1914). The epidermal hydathode is made up of a group of modified epidermal cells, which secrete water or salt out of the leaf through an active process. The epithemal hydathode consists of water pores, epithem, tracheid-ends, and a sheath layer, and its exudation of water is caused by root pressure belonging to the passive type. The water pores are the modified stomata in hydathodes, and they usually are not regulated. The epithem tissue of hydathodes are composed of a mass of sinuous and thin-walled parenchyma cells that act as a filter and have the function of retrieving nutrient solutes during guttation (Klepper and Kaufmann, 1966; Dieffenbach et al., 1980; Sperry, 1983; Canny, 1990; Wilson et al., 1991).

Several reports have indicated several genes expressed in hydathodes—including genes for acidic chitinase, herbicide safener-inducible gene product, pyrroline-5-carboxylate reductase, peroxidase, and the PHO1 proteins—and their functions are related to plant defense and solute transport (Samac and Shah, 1991; de Veylder et al., 1997; Hua et al., 1997; Gay and Tuzun, 2000; Wang et al., 2004). These studies imply that hydathodes might play an important role in nutrient retrieval and plant defense.

Theoretically, a close relationship between the development and function of hydathode for guttation must exist. In other words, the structural differentiation and maturation of the water pores and epithem in the hydathodes are the basis for judging when guttation is working. However, articles about hydathode development have rarely surfaced, and only one has emphasized epithem cell morphogenesis (Galatis, 1988). It asserted that the lobed epithem cell formation is directly related to groups' arrangement of cortical microtubules. Our

*Corresponding author: e-mail: yrc@ntu.edu.tw; Fax: 02-33662478.

previous studies examined the ultrastructure of the laminar hydathodes in *Ficus formosana* (Chen and Chen, 2005). In the present study, we use the techniques of LM, SEM, and TEM to examine the morphogenesis of the hydathodes, with special emphasis on the spatial and temporal differentiation of epithem cells. We have also quantified the area of the hydathode and the number of water pores per hydathode that occur during hydathode development. Such data were provided to illustrate and confirm the relationship between the maturity of hydathodes and the validity period of guttation.

MATERIALS AND METHODS

Plant material

Ficus formosana Maxim. f. *Shimadai* Hayata was planted in pots filled with soil in the greenhouse of the Botany Department, National Taiwan University. Plants were watered daily, and an automatic device recorded temperature and humidity. The growth data for 5-15 successive leaves on the shoot were measured and recorded. All leaf growth data were transferred with the LMI method (Chen et al., 2005), and then regressed by a growth curve with the sigmoid function (Figure 1A). By analyzing the leaf growth curve through the first and secondary differentiation as shown in Figure 1B, two refractive points of the secondary differentiation LMI 3.13 and 8.37 were obtained. Based on these two refractive points, we divided the growth curve into three phases: the log, linear, and stationary phases. We identified four developmental stages: LMI at -1.8 was the initial stage, and three additional leaf growth phases represented the stages of cell division, cell elongation and differentiation, and maturation. These selected samples of the 5-15 successive leaves separated into four developmental stages were collected for light and electron microscopic studies and were shown as the marks in Table 1. Each leaf sample included three pieces taken from the middle region of leaf blade.

Light microscopy

Leaf samples of *F. formosana* containing achlorophyllous hydathodes were fixed with 2.5% glutaraldehyde in 0.1 M sodium cacodylate buffer (pH 7.0) for 6 h at room temperature and then washed in a rinse buffer (0.1 M sodium cacodylate buffer) thrice. Washed materials were post fixed with 1% OsO_4 in 0.1 M cacodylate buffer (pH 7.0) for 8 h at room temperature, washed in 0.1 M sodium cacodylate buffer, and dehydrated in an acetone series and embedded in Spurr's resin (Spurr, 1969). After polymerization of resin at 70°C for 8 h, the plastics were trimmed and prepared for sectioning. For light microscopic observations, plastic sections 0.75 μm thick were cut with glass knives on a Reichert Ultracut E ultramicrotome, stained with 1% toluidine blue, observed under a Zeiss Photomicroscope III, and photographed with Kodak TMAX 100.

Transmission electron microscopy

Ultrathin sections (80 nm in thickness) were cut with a diamond knife and picked up on the formvar-coated 75 mesh grids and double stained with aqueous uranyl acetate for 25 min and lead citrate for 5 min. The stained sections were examined in a Hitachi H-600 transmission electron microscope (TEM) at 75 kV.

Scanning electron microscopy

Sample fixation and buffer washers were performed as described above, dehydrated through an ethanol series up to 100% ethanol, transferred to pure acetone, and critical point-dried in the Hitachi Critical Point Dryer HCP-2. Then, specimens were mounted on aluminum stabs with

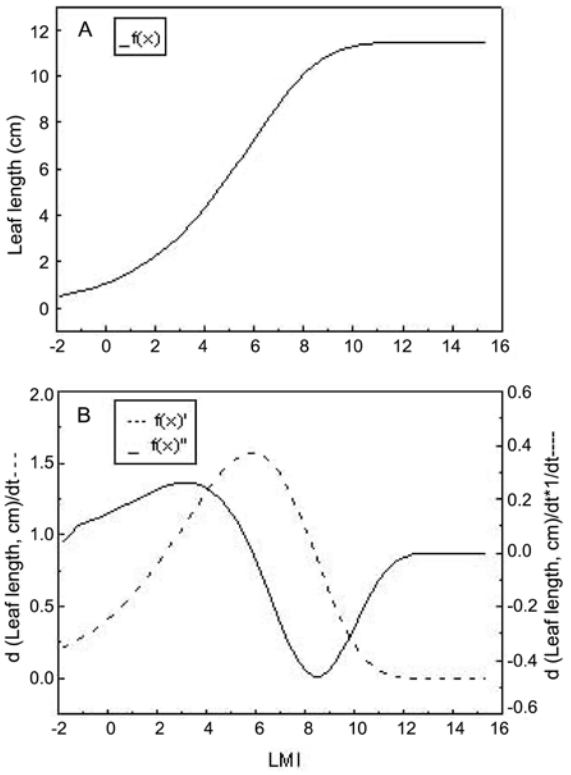

Figure 1. Analysis of the fitted leaf-growth curve of *F. formosana* Maxim. f. *shimadai* Hayata by first and secondary differentiations. A, Best fitted leaf-growth curve regression with the Weibull function f(x); B, Graphs of the first and secondary differentiation. Dash line indicates the graph of first differentiation f(x)'; d (leaf length, cm)/dt plotted against time, and the maximum is 1.57 cm $(LMI)^{-1}$ at 5.57 LMI. Solid line indicates the graph of the secondary differentiation f(x)", d (leaf-length)/dt^2 plotted against time, and the maximum and minimum are 0.26 cm•LMI^{-1} (at 3.13 LMI) and -0.46 cm•LMI^{-1} (at 8.37 LMI), respectively. Figure abbreviations: C, chloroplast; CW, cell wall; E, epithem cell; ER, endoplasmic reticulum; G, Golgi body; H, hydathode; IS, intercellular space; L, laticifer cell; M, mitochondrion; Mt, microtubule; N, nucleus; O, water pore aperture; P, peroxisome; PD, plasmodesmata; PT, palisade tissue; S, starch-containing plastid; SG, salt-glandular trichome; SL, sheath layer; ST, spongy tissue; T, trichome; TC, tracheid cell; V, Vacuole; VB, vascular bundle; WP, water pore.

Table 1. The developmental stages of the tested leaves of *Ficus formosana* Maxim. f. *shimadai* Hayata.

Leaf number (acropetally)	Leaf length (cm)	Leaf measuring-interval index (LMI)	Phase of leaf growth curve	Development stage of hydathode
5*	11.4	14.3	Stationary	Maturation
6*	10.7	13.2	Stationary	Maturation
7	11.2	11	Stationary	Maturation
8	12.2	10	Stationary	Maturation
9*	11.5	8.6	Linear	Cell elongation and differentiation
10	8.8	6.8	Linear	Cell elongation and differentiation
11*	6.3	5.4	Linear	Cell elongation and differentiation
12*	3.1	3.2	Linear	Cell elongation and differentiation
13*	1.8	1.6	Log	Cell division
14*	1.1	0.2	Log	Cell division
15*	0.7	-0.8	Log	Cell division
16*	0.5	-1.8	Log	Initial
17*	0.3	-2.8	Log	Initial

*Leaves were collected for embedding and sectioning.

silver paste, coated with palladium-gold in an ion-sputter coater (Eiko Engineering, Ltd. IB-2 ion coater), and viewed in a Hitachi S-520 SEM.

Cleaning method

Venation was studied with clearing leaves by using the technique of Shobe and Lersten (1967). Leaf blades were first cut to a size of 2 × 1 cm^2, depigmented in 70% ethanol solution, bathed in boiling water for 10 to 30 min, and then placed in 5% aqueous sodium hydroxide at 60 °C until they were partially cleared. Subsequently, they were treated with lactic acid for clearing. Then sections were stained with 1% Safanin O in 50% ethanol for 1 h and destained in 50% ethanol until veins were clearly observable.

Measurement of area of hydathode, length of trichome and the number of water pores on hydathode

Samples were prepared through a clearing method and stained with 1% Safanin O. Based on different developmental leaf stages, cleared samples were used to calculate the area of hydathode, length of a giant trichome nearby, and the number of water pores per hydathode under Nikon light microscopy with the image analysis soft of PC meter.

RESULTS

Four stages of hydathode development Identified

As shown in Table 1, these sample leaves were collected and separated into four development stages: the initial, the cell division, the cell elongation and differentiation, and the maturation stages. Meanwhile, the growth curve of the hydathode area and the number of water pores in each hydathode were obtained (Figures 2, 3). They were sigmoid type, and their growth rates peaked at 3.3 and 4.7 LMI, respectively.

Laminar hydathode development of *F. formosana* observed by SEM

In the early stage of leaf development (-1.8 LMI), the trichome is initially observed as a protuberant cell on the leaf surface (Figures 4A, B). Following this, the slight salient of the hydathode's initial cells is observed near the basal region of the trichome in the later stage (-0.8 LMI; Figure 4C). The distribution of hydathodes occurs not only on the adaxial surface of leaf, but also at the leaf tip (Figures 4D, H). As cell division become more active, the bulge region becomes larger (Figure 4E), and some water pores begin differentiation. In the early cell elongation and differentiation stage (3.2 LMI), the bulge region reaches its maximum height. Afterwards, as the leaf extends, the bulge flattens gradually, and the hydathode's area becomes larger (Figures 4F-G). Water pores are obvious in this stage. In the maturation stage, the salient surface of hydathode accompanying the leaf extension is fully expanded to become flattened and evenly concave (Figure 4I).

As shown in Figure 5, the trichomes grow quickly up to a size over 200 μm in the cell division stage, peaking in size in the cell elongation and differentiation stage of hydathode development (Figures 4E, G). In general, one or two trichomes are present near the laminar hydathodes,

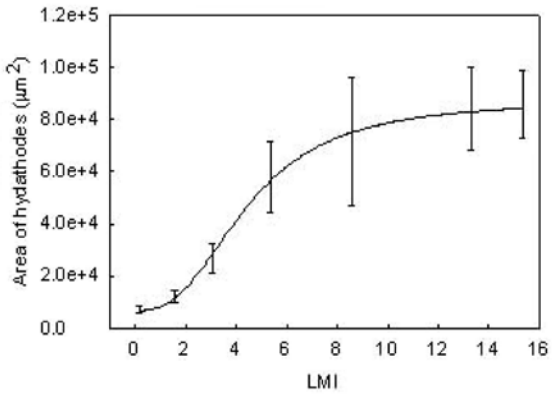

Figure 2. The growth curve of hydathode area of laminar hydathodes on leaves of *F. formosana* Maxim. f. *shimadai* Hayata. (n = 30, r^2 =0.78, $p < 0.05$).

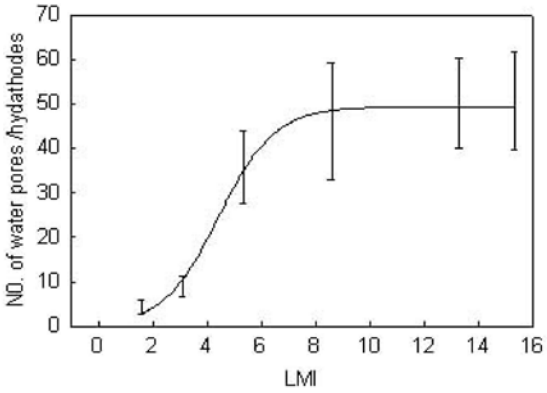

Figure 3. Growth curve of water pore numbers of the laminar hydathodes on leaves of *F. formosana* Maxim. f. *shimadai* Hayata. (n = 30, r^2 = 0.74, $p < 0.05$).

most of one trichome occurs (Figures 4F-H). Besides a giant trichome, many salt glandular trichomes surrounding the surface of laminar hydathodes or leaf-tip hydathode are also observed (Figures 4G, H). These salt glandular trichomes drop gradually in later development, and they are completely lost by the mature stage of hydathodes (Figure 4I). Water pore differentiation could occur through hydathode development (Figure 4E), and this growth curve is shown in Figure 3.

Relationship between hydathodes development and venation

The laminar hydathodes of *F. formosana* belong to the epithemal hydathode type, and they communicate directly with the water-conducting system of leaf. The correlated relationships between the hydathodes and venation during leaf development are shown with clearing-treated leaves (Figure 6). In early stage of leaf venation, the primary and secondary veins are differentiated, and the initial cells of laminar hydathodes are present near the trichomes on the adaxial leaf surface (Figure 6A). Following development (in the cell elongation and differentiation stage), the tertiary veins begin differentiation, and some differentiated water pores are observed on the epidermis of protruding hydathodes (Figure 6B). After leaf expansion, the quaternary veins branch out from the tertiary ones and then differentiate into the epithem, connect with the differentiated tracheid within hydathodes, and finally form clustering vein-ends fusion beneath the water pores at the mature stage (Figures 6C, D). The spatial relationships of water pores, epithem and vascular bundles are shown in Figure 6E and F. The development of epithem cells not only accompanies water pore differentiation, but is also associated with quaternary vein differentiation during hydathode development. The maturation of hydathodes is basipetal, similar to that of venation.

Development of the laminar hydathodes observed by LM

Overviews of the cross-sections of laminar hydathodes at different leaf lengths during leaf development are shown in Figure 7. In the initiation stage, the first significant hydathode differentiation is composed of several enlarging cells near the trichome that proliferate through successive anticlinal divisions in the adaxial epidermis to perform a bulge (Figures 7A, B). In the cell division stage, epidermal cells divide more actively in the anticlinal plane, and irregular anticlinal, mixed with periclinal, divisions in the subepidermal cells produce a large bulge consisting of a mass of cells as the original cells of water pores, epidermis and epithem cells (Figures 7C-E). The division and growth of these cells are behind the bulge morphology of hydathodes on adaxial leaf surface. After the cell division stage, hydathodes enter the elongation and differentiation stage (Figures 7F, G). In this stage, water pore mother cells continue to divide and differentiate, and epithem cells begin to grow, and intercellular spaces start to form. During tissue expansion, epithem cells grow into lobed shapes with sinuous cell walls and intercellular spaces among them similar to spongy mesophyll cells. A sheath, one cell layer thick, surrounds the epithem and connects with the bundle sheath and epdermis (Figure 7H). When the leaf reaches full expansion, water pores are present on the surface of the hydathodes, and the lobed epithem cells are in contact with conspicuous intercellular spaces, and the vascular bundles are surrounded by a sheath layer (Figure 7I).

Ultrastucture of epithem of laminar hydathodes at initial and cell division stages

The initiation of hydathodes begins from a large epidermal cell near a giant trichome, and it undergoes a series of specialized anticlinal divisions to produce a group of cells that protrude slightly from the epidermis. At this stage, these cells have a large nucleus, dense cytoplasm containing large numbers of small vesicles, and many plasmodesmata present on the cell wall between cells (Figures 8A, B). Following cell division, the original cells of epidermal layer proliferate through asymmetrically anticlinal division to form the meristemoid mother

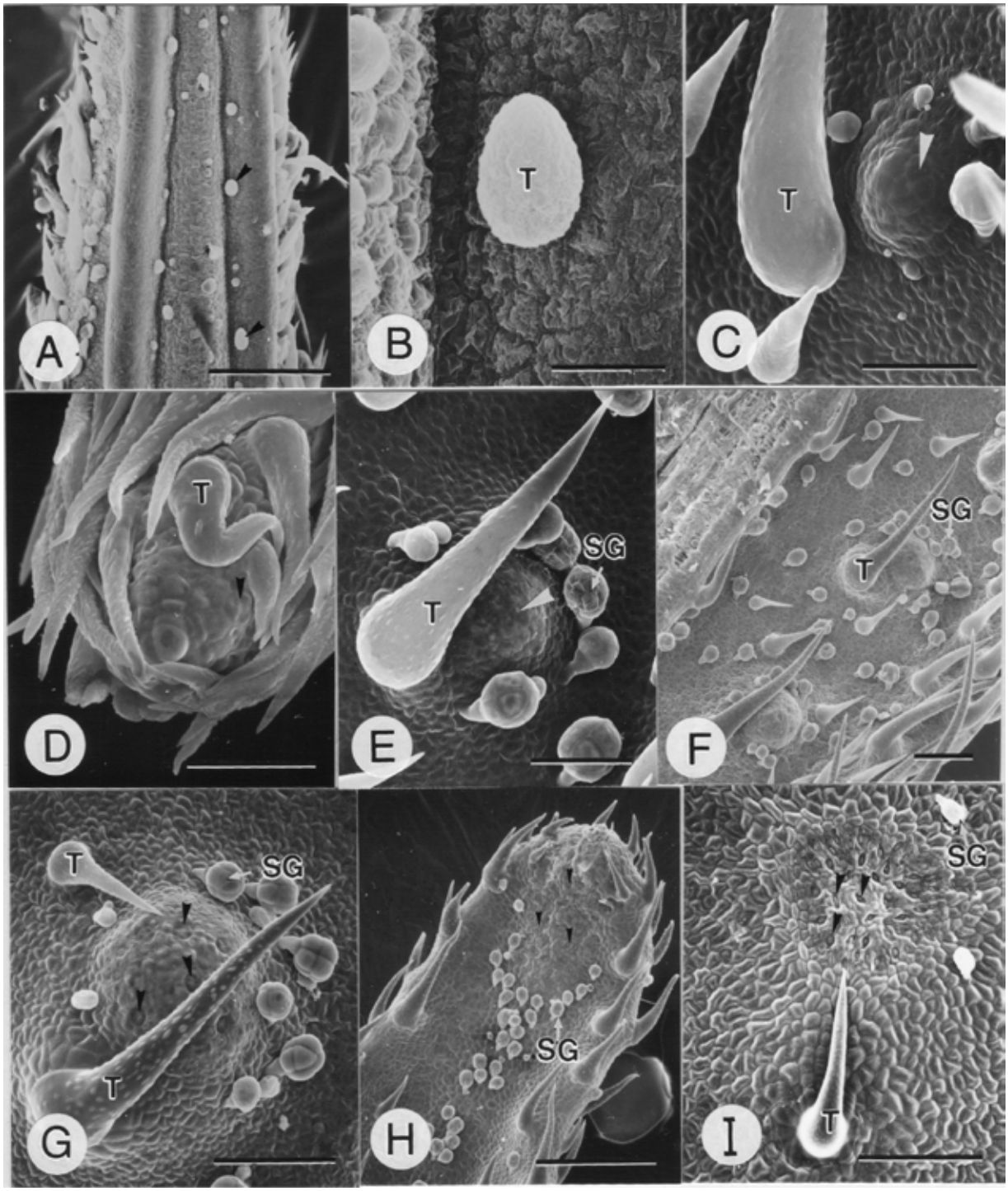

Figure 4. SEM micrographs showing morphology of laminar hydathodes at different developmental stages on leaves of *F. formosana* Maxim. f. *shimadai* Hayata. A, During early log phase stage, -1.8 LMI, the trichome initial can be observed on adaxial surface of leaf (arrowheads); bar scale is 75 μm; B, Larger magnification of the trichome initial cell in the Figure 1A; bar scale is 10 μm; C, During log phase stage, 1.6 LMI, a hydathode initial is observed on the adaxial surface of leaf (arrowhead), and a giant trichome is nearby protecting it; bar scale is 50 μm; D, Hydathodes are on the leaf tip at 1.6 LMI. Arrowhead indicates water pore in differentiation; bar scale is 100 μm; E, Laminar hydathode on the leaf stage at 1.6 LMI. The water pores are differentiated, and several salt glandular trichomes and a giant trichome surround it; bar scale is 50 μm; F, External feature of hydathodes the early linear phase stage at 3.2 LMI. Two laminar hydathodes can be observed; bar scale = 100 μm; G, External feature of the hydathode at 5.4 LMI, several water pores are differentiated and matured (arrowheads); bar scale is 75 μm; H, External features of the hydathode on the leaf-tip with stage at 5.4 LMI; there are many salt glandular trichomes surrounding the hydathode; bar scale is 200 μm; I, Water pores on the surface of a hydathode in the mature stage at 13.2 LMI. A giant trichome and two residual salt glandular trichomes surrounding it; bar scale is 120 μm.

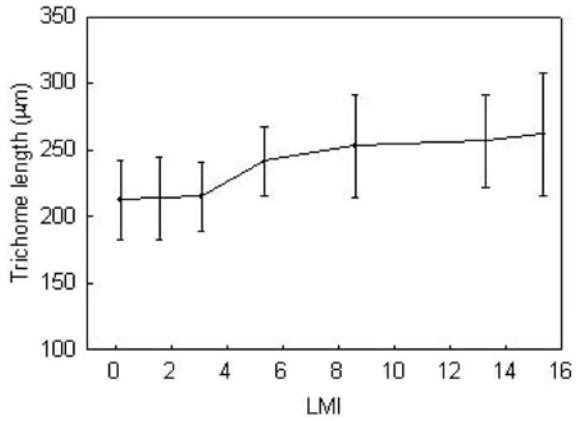

Figure 5. Growth curve of trichomes nearby laminar hydathode on leaves of *Ficus formosana* Maxim. f. *shimadai* Hayata. (n = 30, mean value ± SD, $p < 0.05$)

cells and epidermal cells; the subepidermal cells further undergo irregular anticlinal and periclinal divisions to form original cells of epithem, which are characterized by thin cell walls, chloroplasts, and small vacuoles (Figures 8C, D). At this moment, some tracheids are differentiated in the lower region of the epithem.

Ultrastructure of epithem of laminar hydathodes at cell elongation and differentiation stages

In the early phase of the cell elongation and differentiation stage, the meristemoid on the epidermis grows larger, becomes a water pore mother cell, and further symmetrically divides into the guard cell pair. The water pore mother cell on the epidermis is characterized by a large nucleus, dense cytoplasm, and a large number of small vesicles in the cytoplasm (Figure 9A).

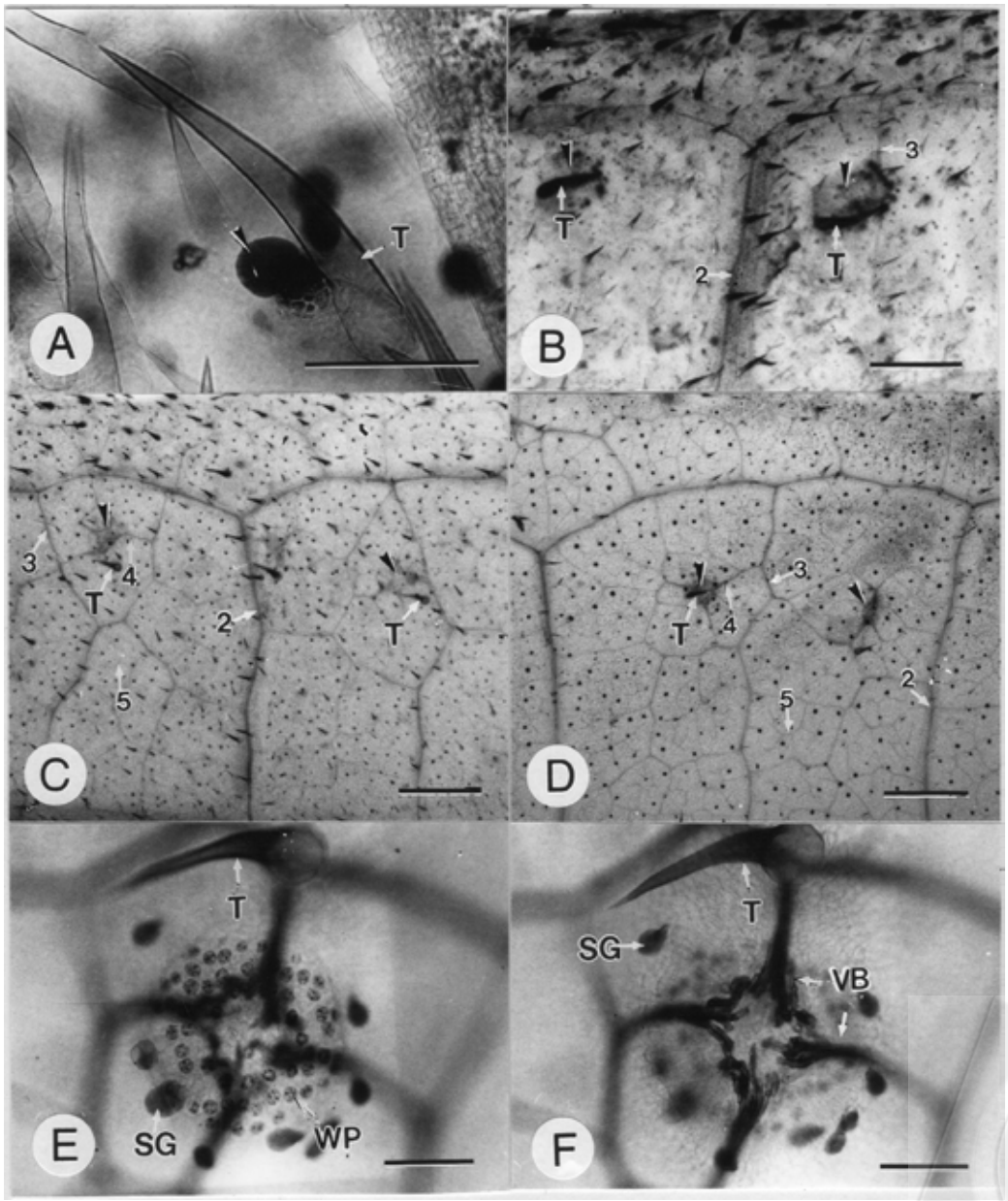

Figure 6. Light micrographs of laminar hydathodes on clearing-treated leaves of *F. formosana* Maxim. f. *shimadai* Hayata at different developmental stages. A, Enlargement of a hydathode (arrowhead) on leaf at 1.6 LMI; bar scale is 100 μm; B, Two hydathodes (arrowheads) and tertiary vein beginning differentiation in leaf at 3.2 LMI; bar scale is 100 μm; C, Differentiated quaternary veins and differentiating fifth veins in leaf at 5.4 LMI. Arrowheads indicate hydathodes; bar scale is 1 mm; D, Differentiated finest veins and full venation in leaf at 13.2 LMI. Arrowheads indicate hydathodes; bar scale is 1 mm; E-F, Hydathode at 8.6 LMI; E, Surface of a laminar hydathode showing a group of water pores; bar scale is 100 μm; F, Section view at tracheary elemental level showing several tracheid-ends fusing together from four vascular bundles in the epithem of a hydathode, bar scale is 100 μm.

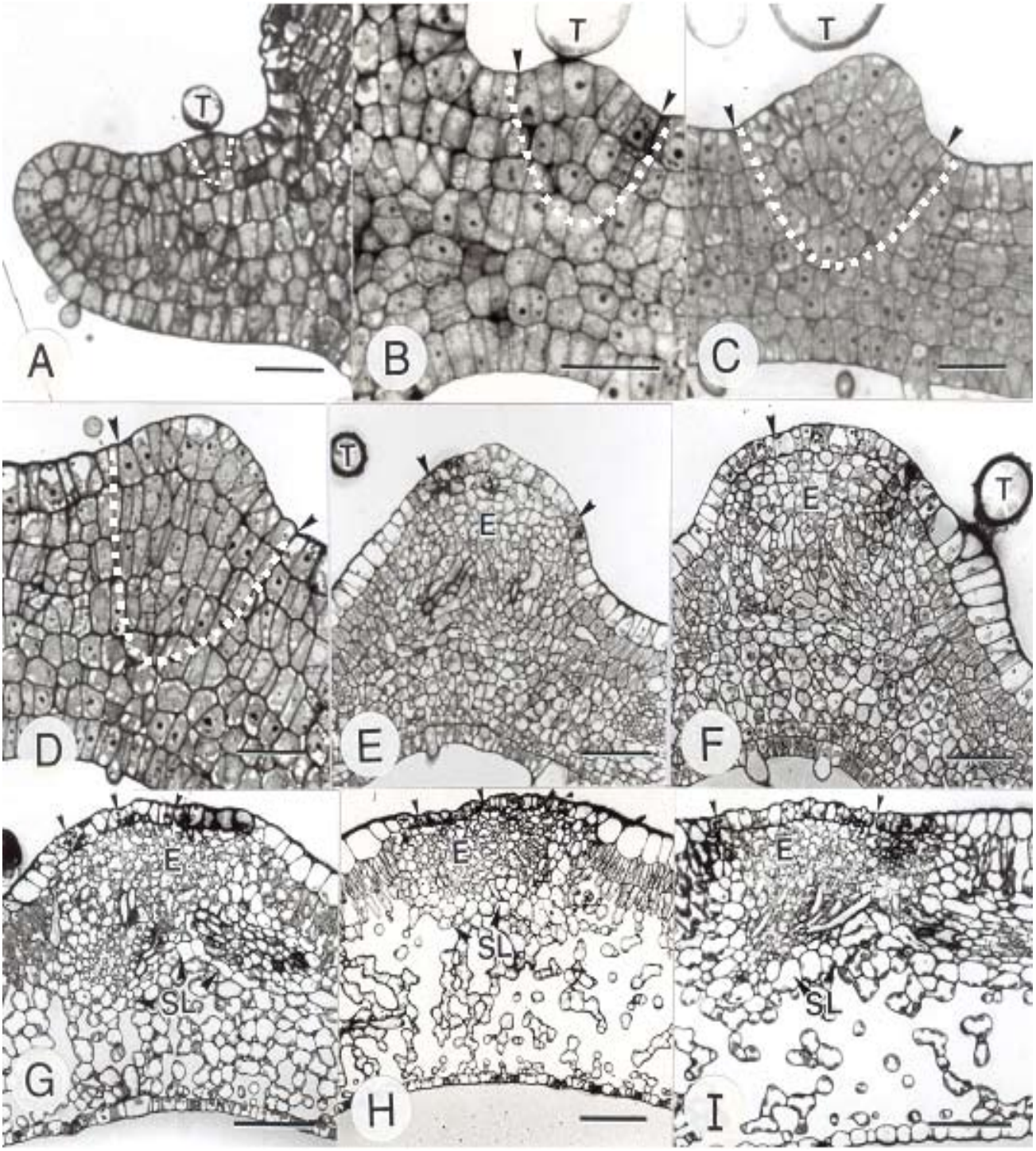

Figure 7. Light micrographs of laminar hydathodes at different development stages on leaves of *F. formosana* Maxim. f. *shimadai* Hayata. A, A hydathode at initial stage at -1.8 LMI. Protruded region nearby a trichome is the hydathode initial; B-D, Cross sections of hydathodes at cell division stage. The region indicated by two arrows shows anticlinal division in epidermis, and white dotted line surrounding region are irregular anticlinal and periclinal division; B, Hydathode at -0.8 LMI; C, Hydathode at 0.2 LMI; D, Hydathode at 1.6 LMI; E-G, Cross sections of hydathodes at cell elongation and elongation stage; E, Hydathode at 3.2 LMI; arrowheads indicate water pores; F, Hydathode at 5.4 LMI. Arrowhead indicates the longitudinal section of the mature water pore; G, Hydathode at 8.6 LMI; H-I, Cross sections of hydathodes at maturation stage; H, Hydathode at 13.2 LMI. Arrowheads indicate the water pores; I, Hydathode at 14.3 LMI. Arrowheads indicate the water pores. A-D, bar scales are 25 μm; E-I, bar scales are 50 μm.

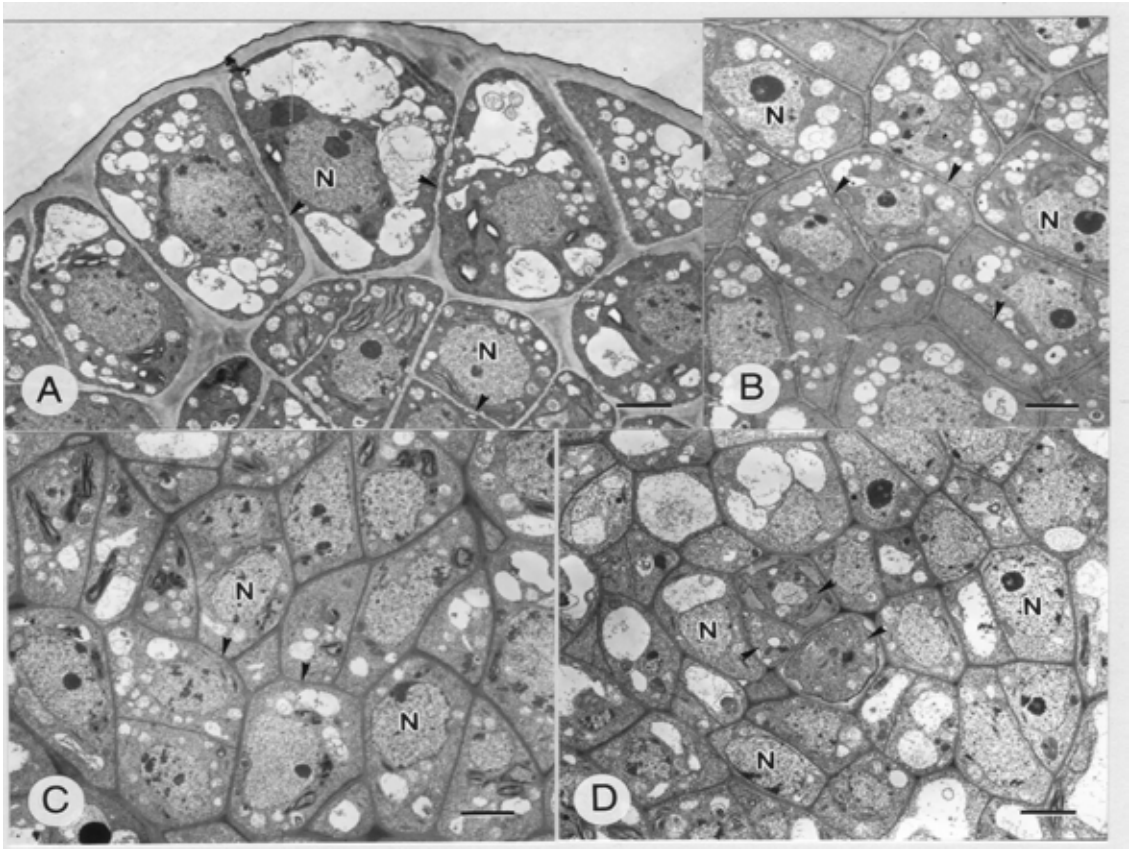

Figures 8. TEM micrographs showing epithem development in leaves of *F. formosana* Maxim. f. *shimadai* Hayata in the initial and the cell division stages. A, Cross section of hydathodes in the initial stage at -0.8 LMI. Arrowheads indicate plasmodesmata; B, Paradermal section of a hydathode in the early cell division stage at -0.8 LMI. Arrowheads indicate plasmodesmata; C, Cross section of a hydathode showing the upper region of epithem in the late cell division stage at 0.2 LMI. Arrowheads indicate plasmodesmata; D, Cross section of a hydathode showing the lower region of epithem in the late cell division stage at 0.2 LMI. Arrowheads indicate tracheid cells are in differentiation. All bar scales are 2.5 μm.

In the cell elongation and differentiation stage, epithem cells gradually grow and begin to schizogeny, starting from the subepidermal region towards the vein-ends (Figures 9B, C). Some digested materials are observed in the middle lamella, and the lobe-shaped epithem cells and the intercellular spaces are formed. At the same time, the intercellular space remains unformed in the middle region of the epithem (Figure 9D). Several differentiated tracheids were also observed among epithem cells (Figures 9E). In addition, a sheath layer surrounds the epithem and extends toward the epidermis. The cellular characteristics of sheath layer cells are a normal appearing nucleus, a large vacuole preferentially located on the proximal side toward epithem, and the major organelles present in the cytoplasm at the distal side from epithem (Figure 9F).

Following development, the epithem cells grow more elongated and lobed, and their intercellular spaces are extended more obviously. Epithem cells are characterized by a sinuous cell wall and abundant organelles, including mitochondria, Golgi, ER, ribosomes, peroxisomes, plastids and many small vacuoles in the cytoplasm (Figures 10A-C). Intercellular space is gradually formed from water pores to tracheid-ends. In differentiated tracheids, many dictyosomes and their derivate vesicles are secreted outward from the cells for secondary wall thickening (Figure 10D). The schizogenous process of intercellular space formation in the epithem is shown in Figures 10E-G. Epithem cells containing several Golgi vesicles accumulated near the cell wall, and many electron dense materials are observed in the middle lamella (Figures 10E-F). Meanwhile, cortical microtubules have also been observed in the inside region of the sunken wall of epithem cells (Figure 10G).

Ultrastructure of epithem of laminar hydathodes at maturation stage

At the mature stage of laminar hydathodes, the epithem consists of the large and lobed cells contacted with extensive intercellular spaces, and many plasmodesmata present on the contacted cell wall (Figures 11A-C, F). The sheath layer cells have a large central vacuole, with the cytoplasm and other organelles located in the pericytoplasm of cells (Figure 11D). The cytological characteristics of epithem cells are many small vacuoles fusing to form several larger ones, and the numbers of peroxisomes per cell obviously increase as cells mature (Figures 11E, F).

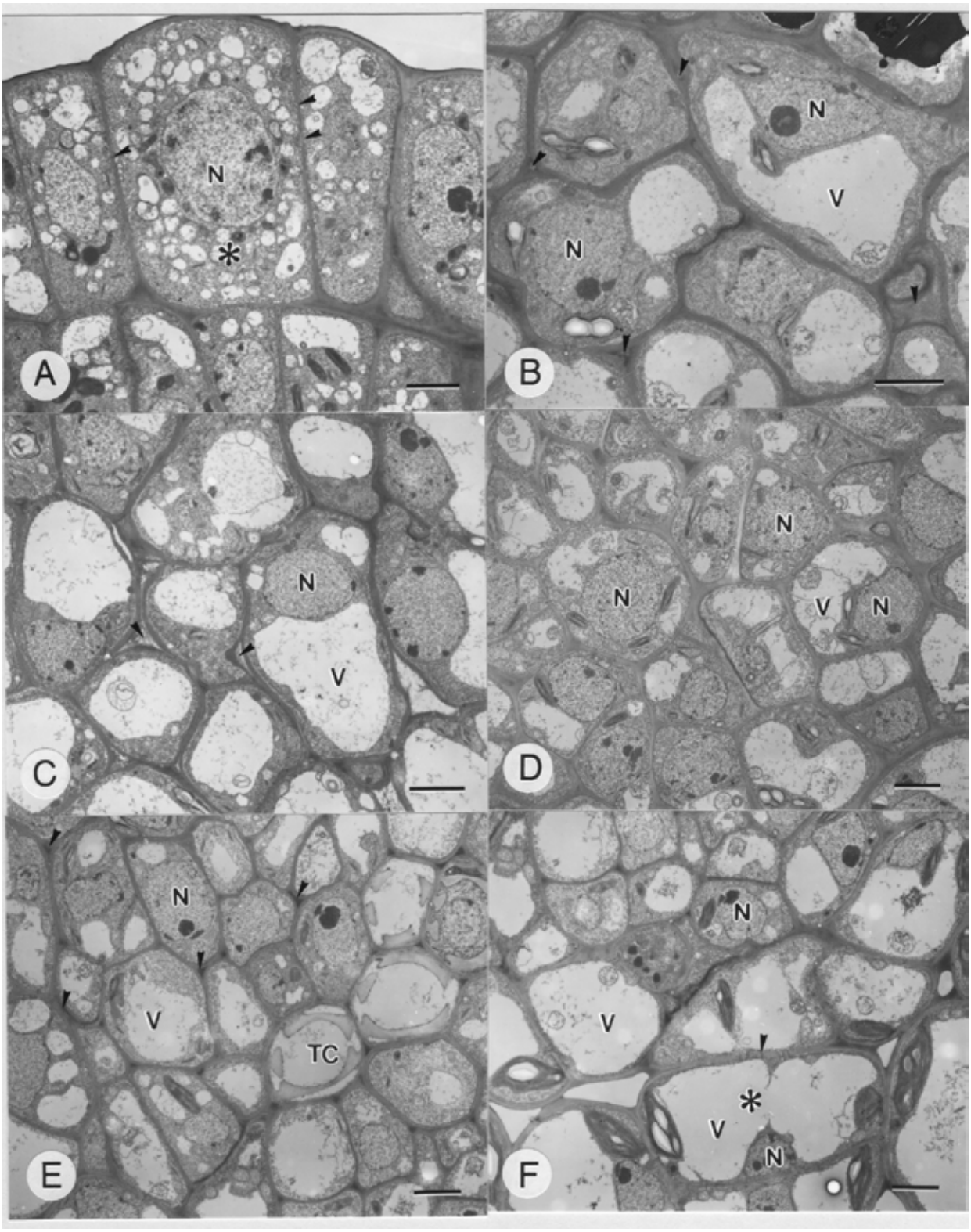

Figure 9. TEM micrographs showing epithem development in leaves of *F. formosana* Maxim. f. *shimadai* Hayata in early phase of cell elongation and differentiation stages at 3.2 LMI. A, A hydathode showing meristemoid mother cell of a water pore in epidermis (asterisk). Arrowheads indicate plasmodesmata; B, Epithem cells under epidermis. Arrowheads indicate the sites of digested materials in the intercellular space; C, Epithem cells under the subepidermal region. Arrowheads indicate the intercellular space; D, Epithem cells in the middle region of a hydathode; E, Epithem cells in the lower region of a hydathode. Arrowheads indicate the intercellular space formation; F, The sheath layer nearby epithem was labeled by asterisk Arrowhead indicates plasmodesmata. All bar scales are 2.5 μm.

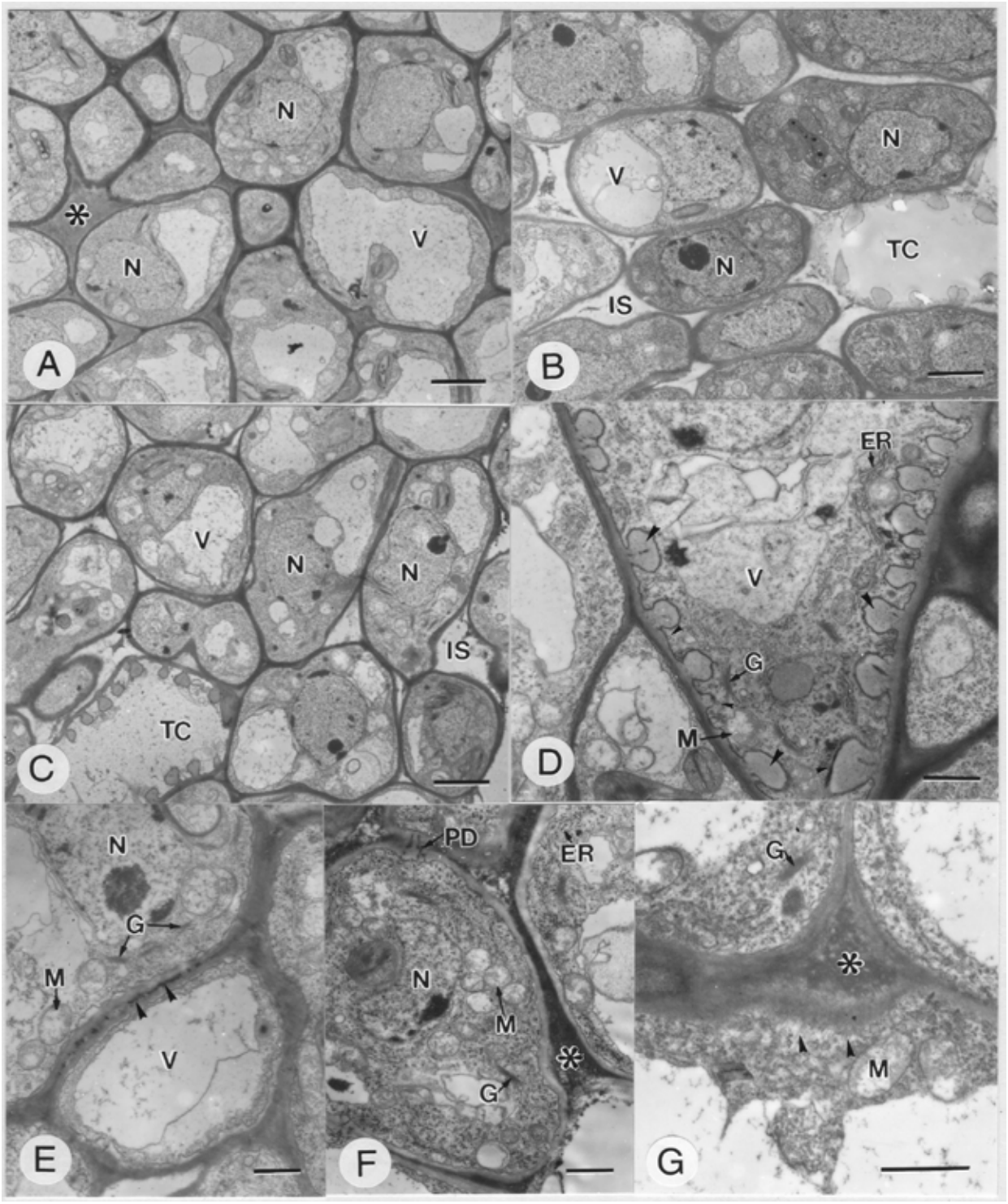

Figure 10. TEM micrographs showing epithem development in leaves of *F. formosana* Maxim. f. *shimadai* Hayata in the middle phase of cell elongation and differentiation stage at 5.4 LMI. A, Epithem cells in the upper region of hydathodes. Asterisk indicates the lyses of middle lamella for performing intercellular spaces between epithem cells; B, Epithem cells in the middle region of hydathodes; C, Epithem cells in lower region of hydathodes; D, A tracheid cell in differentiation stage showing many Golgi apparatuses and secretary vesicles in their cytoplasm. Arrowheads indicate the thickening cell wall of a tracheid cell. Small arrowheads indicate vesicles fused with secondary wall; E, Lysogeneous cell wall initially formed between two epithem cells. Arrows indicate the sites of lysogensis; F, Lysogenous cell wall formed between two epithem cells for formation of intercellular spaces. Asterisks indicate the formation of intercellular space; the electron materials are the lyses materials; G, Lysogenous cell wall among epithem cells for formation of intercellular space. Asterisk indicates the formation of intercellular space; the electron materials are the lyses materials and arrowheads point microtubules present in the pericytoplasm of epithem cell. A-C, bar scales are 2.5 μm; D-G, bar scales are 1 μm.

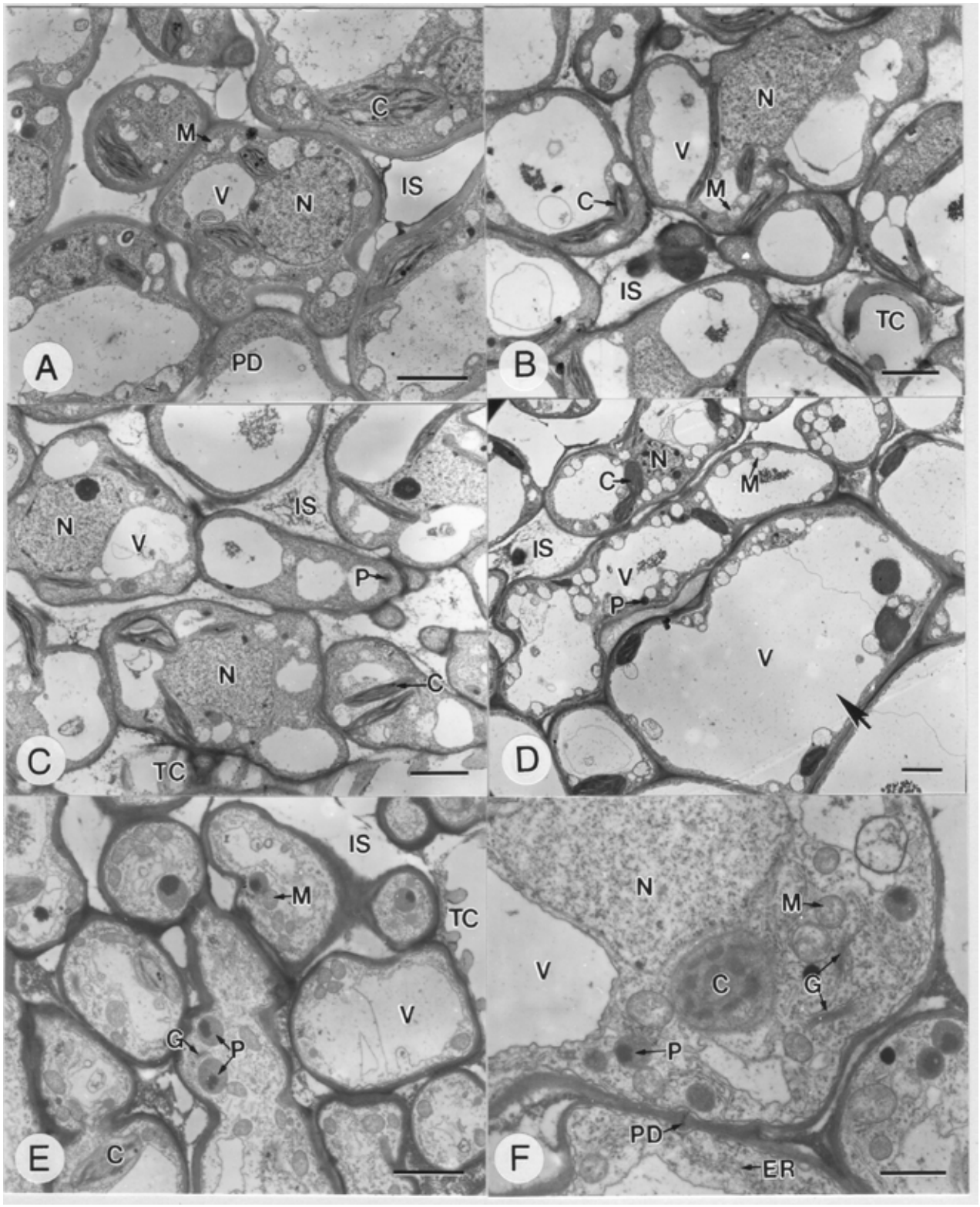

Figure 11. TEM micrographs showed epithem development in leaves of *F. formosana* Maxim. f. *shimadai* Hayata in the maturation stage at 13.2 LMI. A, Cross section of epithem under epidermis; B, Cross section of epithem in the middle region of a hydathode; C, Cross section of epithem in the lower region of hydathodes nearby the tracheid cells; D, Cross section of epithem near the sheath layer. Arrow indicates a sheath layer cell; E, Mature epithem cells; F, Partial magnification of mature epithem cell. A-E, bar scales are 2.5 μm; F, bar scales are 1 μm.

DISCUSSION

Initial and development of laminar hydathodes associated with venation

The initial hydathode site is specified early in leaf development and corresponds to the formation of a giant laminar trichome. It is also related to the tracheid differentiation associated with the venation development. Similar phenomena were also observed in Urticaceae (Smith and Watt, 1986; Lersten and Curtis, 1991). Aloni et al. (2003) studied the role of auxin in the vascular differentiation and leaf morphogenesis of *Arabidopsis*. They observed that hydathodes developed in the tip and leaf teeth, thatthe process of auxin-conjugate hydrolysis apparently produced primary sites of high free-auxin, and that trichomes and mesophyll cells were secondary sites of free-auxin production. During primordial development, gradual changes in the sites and concentrations of free-auxin production occurred first in the tip of a leaf primordium, progressively and basipetally shifting along the margins before finally appearing in the central regions of the lamina. This developmental pattern of free-auxin production was suggested to control the basipetal maturation sequence of leaf development and vascular differentiation in *Arabidopsis* leaves. The distribution of trichomes and hydathodes could also affect the venation pattern in different plants. In the present study, hydathode initials usually appear near the giant trichomes on the adaxial leaf surface. The above may indicate that auxin produced by trichomes possibly induces tracheid differentiation and the initiation of hydathodes. Laminar hydathodes form at the junction of the quaternary vein-ends, and they are confirmed to belong to the epithemal hydathodes (Figure 4D-F).

Schizogenous intercellular space performing during epithem differentiation

In the third stage of hydathode development, epithem cells begin to enlarge and to differentiate after cell division. A special organization pattern of cortical microtubules and the hydrolytic activity of the cell-wall digest enzymes together and form the lobed shape and conspicuous intercellular spaces (Galatis, 1988; Apostolakos et al., 1991). The formation of intercellular spaces is first performed by enzyme digestion of pectin in the middle lamella of epithem cells, a process the pectinase might be involved in (Li et al., 2004). At the same time, turgor pressure provides non-woody plant tissues with mechanical rigidity and the driving force for growth, and also generates large forces tending to the separation of cells (Jarvis et al., 2003). The irregular cluster pattern of microtubules favors the lobe-walled formation (Galats, 1988). This special arrangement of microtubules might be induced by salt stress (Komis et al., 2002). The lobed cell formation of intercellular space in the epithem belongs to the schizogenous type that is different from other aerenchyma formations of leaf spongy tissues, which contain both schizogenous and lysigenous mechanisms (Evans, 2004). Why do epithem cells form a lobed shape that is different from the palisade cells nearby? We suggest that the lobe-shaped epithem might be caused by salt stress, which induced the cortical microtubule to group's arrangement.

Period of guttation based on stages of hydathode development

Analyzing the growth curves of the hydathode area and the number of water pores associated with the ultrastructural data of epithem cells and water pores that could be used to illustrate and judge the guttation period of hydathodes. The extension rate of the hydathode's area reached a maximal value, 36 μm (LMI)-1, at 3.3 LMI. The water pores gradually mature within from 0.2 to 8.0 LMI. Their numbers increasing rate reached maximal value, 14 (LMI)-1, at 4.7 LMI (Figure 3). During the early stage at 1.6 LMI, guttation of hydathodes was not observed even though some water pores were mature, but the epithem and tracheary elements were in the cell division stage. Guttation happens in the later stage of leaf development of *F. formosana*. Smooth guttation must theoretically be based on hydathode maturity, especially the intercellular space formation and water pore and tracheid-end maturation. So, the role of salt-glandular trichomes in the early stage of leaf development is very important for eliminating excess salt in the xylem saps of the hydathode. Actually, the tip-hydathode matures and functions early in the linear phase of leaf development at 3.1 LMI. Afterward the laminar hydathode function is gradual and basipetal.

In Saxifraga, the total quantity of guttation is related to the developmental stage of the plant, and hydathodes excrete water only at a definite developmental stage (Schmidt, 1930). In *Zea mays* and *Canna indica*, hydathodes are formed at very early stages of leaf development, and guttation has been observed at this stage (Höhn, 1950). However, the rate of water excretion from these leaves is low because the young developing leaves are densely packed in the buds. The highest guttation activity occurs during unrolling of the leaves and vigorous growth of the plant.

In Caltha, the marginal hydathodes of the leaf function within the bud and for a short time after the leaf emerges from its sheath. Soon after, the epithem and water-pores become filled with a gummy brown material and cease functioning (Stevens, 1956). A similar phenomenon was also observed in our studies; the hydathode surfaces become brown and accumulate much salt incrustation, as well as fungal hypha growth on the older leaves. These materials plug the water pores or the pathway of water to reduce the guttation. Moreover, epicuticular waxes and substances excreted through the hydathodes are occasionally covered with a shield-like plate by which occlusion of water pores prevent guttation in older strawberry leaves (Takeda et al., 1991).

Acropetal mass flow of water is demonstrated in two submerged angiosperms, *Lobelia dortmanna* L. and

Sparganium emersum Rehman by means of guttation measurements (Pedersen, 1993). Transpiration is absent in truly submerged plants, but the presence of guttation verifies that long distance water transport takes place, and the highest rates of guttation occur in young leaves. In addition, some aquatic plants possess an efficient transport system for acropetal translocation of inorganic macronutrients and hormones, and this system is influenced by the developmental stage of the leaf hydathode (Pedersen et al., 1997). The hydraulic properties of the submerged plant, *Sparganium emersum*, have been examined. In leaves with intact leaf tips, the hydraulic conductance per unit length (Kh) is significantly greater in the youngest leaves, and this suggests that the leaf tip with the hydathode influences resistance and thus flow. A matrix of microorganisms develops in the older leaves and probably restricts water flow by clogging the hydathodes.

From the above discussions, we conclude that guttation is related to the leaf development of plants, especially the xylem conduct system, which supports their nutrient demands. Guttation happens in various ways, based on the maturation of the epithem and water pores. The simple hydathodes have fewer or no epithem tissues (most monocotyledons and some dicotyledons), so that guttation usually occurs early in leaf development; however, in the complex hydathodes with intact epithem tissue (most dicotyledons) guttation depends on epithem maturity and water pore formation. Moreover, the hydathodes of monocotyledon occur on the leaf tip, and their leaf development differs from that of dicotyledon. Tip-hydathodes of monocotyledon maturate in early leaf development, and this shows that guttation acts in monocotyledon earlier than in dicotyledon. Following leaf maturation, guttation is be prevented by salt incrustations and microorganism action clogging the hydathodes.

A giant trichome has a protective role at an early stage of hydathode development

Plant trichomes occur in multiple forms and have many functions, including maintaining water balance, secretion of a variety of secondary metabolites and plant defense, especially as a form of physical resistance (Levin, 1973). Figure 5 shows that the trichome length grows up to 80% of its mature length at the earlier stage of hydathode development, and it covers the width of hydathode. We suggest that a giant acicular trichome functions as a physical shelter to protect the hydathodes, especially the protuberant tissue on the leaf surface during early development. Such a shelter function is becomes less important after the maturation of hydathodes in expanded leaves.

LITERATURE CITED

Aloni, R., K. Schwalm, M. Langhans, and C.I. Ullrich. 2003. Gradual shifts in sites of free-auxin production during leaf-primordium development and their role in vascular differentiation and leaf morphogenesis in *Arabidopsis*. Planta **216:** 841-53.

Apostolakos, P., B. Galatis, and E. Panteris. 1991. Microtubules in cell morphogenesis and intercellular space formation in *Zea mays* leaf mesophyll and *Pilea cadierei* epithem. J. Plant Physiol. **137:** 591-601.

Canny, M.J. 1990. What becomes of the transpiration stream? New Phytol. **114:** 341-368.

Chen, C.C., H. Chen, and Y.R. Chen. 2005. New leaf age measurement method: leaf measuring-interval index (LMI). Amer. J. Bot. (In press).

Chen, C.C. and Y. R. Chen. 2005. Study on laminar hydathodes of *Ficus formosana* (Moraceae). I. Morphology and ultrastructure. Bot. Bul. Acad. Sin. **46:** 205-215.

De Boer, A.H. and V. Volkov. 2003. Logistics of water and salt transport through the plant: structure and functioning of the xylem. Plant Cell Environ. **26:** 87-101.

De Veylder, L., M. van Montagu, and D. Inze. 1997. Herbicide safener-inducible gene expression in *Arabidopsis thaliana.* Plant Cell Physiol. **38:** 568-77

Dieffenbach, H., D. Kramer, and U. Lüttge. 1980. Release of guttation fluid from passive hydathodes of intact barley plants. I. Structural and cytological aspects. Ann. Bot. **45:** 397-401.

Evans, D.E. 2004. Aerenchyma formation. New Phytol. **161:** 35-49.

Galatis, B. 1988. Microtubules and epithem-cell morphogenesis in hydathodes of *Pilea cadierei*. Planta **176:** 287-297.

Gay, P.A. and S. Tuzun. 2000. Involvement of a novel peroxidase isozyme and lignification in hydathodes in resistance to black rot disease in cabbage. Can. J. Bot. **78:** 1144-1149.

Haberlandt, G. 1914. Physiological Plant Anatomy. Engl. Trans. London.

Höhn, K. 1950. Untersuchungen über hydathoden und function. Akad. Wiss. Lit. Mainz, Abh. Math.-Nat. Kl. Nr. **2:** 9-42.

Hua, X.J., B. van de Cotte, M. van Montagu, and N. Verbruggen. 1997. Developmental regulation of pyrroline-5-carboxylate reductase gene expression in *Arabidopsis*. Plant Physiol. **114:** 1215-24.

Jarvis, M.C., S.P.H. Briggs, and J.P. Knox. 2003. Intercellular adhesion and cell separation in plants. Plant Cell Environ. **26:** 977-989.

Klepper, B. and M.R. Kaufmann. 1966. Removal of salt from xylem sap by leaves and stems of guttating plants. Plant Physiol. **41:** 1743-1747.

Komis, G., P. Apostolakos, and B. Galatis. 2002. Hyperosmotic stress-induced actin filament reorganization in leaf cells of *Chlorophyton comosum*. J. Exp. Bot. **53:** 1699-1710.

Li, A.M., Y.R. Wang, and H. Wu. 2004. Cytochemical localization of pectinase: the cytochemical evidence for resin ducts formed by schizogeny in *Pinus massoniana*. Acta Bot. Sin. **46:** 443-450.

Lersten, N.R. and J.D. Curtis. 1991. Laminar hydathodes in

Urticaceae - Survey of tribes and anatomical observations on *Pilea pumila* and *Urtica dioica*. Plant Syst. Evol. **176:** 179-203.

Levin, D.A. 1973. The role of trichomes in plant defense. Q. Rev. Biol. **48:** 3-15.

Pedersen, O. 1993. Long-distance water transport in aquatic plants. Plant Physiol. **103:** 1369-1375.

Perdersen, O., L.B. Jorgensen, and K. Sand-Jensen. 1997. Through-flow of water in leaves of a submerged plant is influenced by the apical opening. Planta **202:** 43-50.

Samac, D.A. and D.M. Shah. 1991. Developmental and pathogen-induced activation of the *Arabidopsis* acidic chitinase promoter. Plant Cell **3:** 1063-1072.

Schmidt, L. 1930. Zur funkton der hydathoden von *Saxifraga*. Planta **10:** 314-344.

Shobe, W.R. and N.R. Lersten. 1967. A technique for clearing and staining gymnosperm leaves. Bot. Gaz. **128:** 150-152.

Smith, D.L. and W.M. Watt. 1986. Distribution of lithocysts, trichomes, hydathodes and stomata in leaves of *Pilea-Cadierei* Gagnep and Guill (Urticaceae). Ann. Bot. **58:** 155-166.

Sperry, J.S. 1983. Observations on the structure and function of hydathodes in *Blechnum lehmannii*. Amer. Fern J. **73:** 65-72.

Spurr, A.R. 1969. A low-viscosity epoxy resin embedding medium for electron microscopy. J. Ultrastruct. Res. **26:** 31-43.

Stevens, A.B.P. 1956. The structure and development of hydathodes of *Caltha palustris*. New Phytol. **55:** 339-345.

Takeda, F., M.E. Wisniewski, and D.M. Glenn. 1991. Occlusion of water pores prevents guttation in older strawberry leaves. J. Am. Soc. Hortic. Sci. **116:** 1122-1125.

Tanner, W. and H. Beevers. 2001. Transpiration, a prerequisite for long-distance transport of minerals in plants? Proc. Natl. Acad. Sci. USA **98:** 9443-9447.

Wang, Y., C. Ribot, E. Rezzonico, and Y. Poirier. 2004. Structure and expression profile of the *Arabidopsis* PHO1 gene family indicates a broad role in inorganic phosphate homeostasis. Plant Physiol. **135:** 400-411.

Wilson, T.P., M. J. Canny, and M.E. McCully. 1991. Leaf teeth, transpiration and the retrieval of apoplastic solutes in balsam poplar. Physiol. Plant. **83:** 225-232.

細葉天仙果葉部泌水器的研究：II. 泌水器的形態發育

陳淇釧　陳榮銳

國立台灣大學 分子與細胞生物學研究所

本研究藉由透明法、光學顯微鏡術、掃描與穿透電子顯微鏡術，觀察細葉天仙果葉部泌水器的發育過程，並且著重於描述末梢組織的發育。為了方便說明各發育階段的特色，葉部泌水器發育過程依葉片生長曲線分析將它區分定義為始原細胞期、細胞分裂期、細胞伸長與細胞分化期、及成熟期等四個階段。葉片發育初期，泌水器始原細胞開始出現於葉片上表面的巨大毛茸細胞附近；接著該始原細胞進行細胞分裂，藉由表皮層細胞的垂周分裂形成日後表皮細胞與水孔細胞，次表皮層細胞進行不規則的垂周與平周分裂形成一群細胞團，日後分別分化形成末梢組織、管胞與束鞘細胞層。待發育階段進入細胞生長與分化期，末梢組織的細胞因細胞內細胞質周圍特殊微小管排列的方向、細胞分泌的細胞壁分解酵素其作用及細胞伸長作用產生的張力作用等因子交互作用，使得末梢細胞生長呈成特別的多裂形狀，並且擴大了細胞間的細胞間隙；同時細胞的多裂形狀增加了細胞與其外界環境的接觸面積。此時期的管胞亦進行分化，另外表皮水孔細胞的細胞數目增加速率達到最大。隨著發育階段進入成熟期，末梢組織中的管胞逐漸成熟且具有導水功能，加上末梢組織與水孔成熟的配合，維管束末端管胞到水孔孔口的路徑得以暢通，泌溢作用更順利進行。有趣的是有關末梢組織的分化與成熟具有其方向性，從表皮水孔下方區域逐漸向內近管胞末端區域成熟，所以等到近管胞末端的末梢細胞分化成熟時泌溢作用更明顯易見。本研究結果就解剖學為泌溢作用研究提供了構造學基礎。

關鍵詞：末梢組織；細葉天仙果；泌水器；形態發生；裂生型細胞間隙；水孔。